

**Viscoelasticity of ambient-temperature nematic binary mixtures of bent-core and rodlike molecules**P. Sathyanarayana,<sup>1</sup> V. S. R. Jampani,<sup>2</sup> M. Skarabot,<sup>2</sup> I. Musevic,<sup>2</sup> K. V. Le,<sup>3</sup> H. Takezoe,<sup>3</sup> and S. Dhara<sup>1,\*</sup><sup>1</sup>*School of Physics, University of Hyderabad, Hyderabad 500046, India*<sup>2</sup>*J. Stefan Institute, Jamova 39, SLO-1000 Ljubljana, Slovenia*<sup>3</sup>*Department of Organic and Polymeric Materials, Tokyo Institute of Technology, 2-12-1-S8-42 O-okayama, Meguro-ku, Tokyo 152-8552, Japan*

(Received 21 October 2011; published 11 January 2012)

We report measurements of the temperature variations of physical parameters in ambient-temperature nematic liquid crystal mixtures of bent-core (BC) and rodlike molecules (5CB): birefringence  $\Delta n$ ; static dielectric constants  $\epsilon_{\parallel}$  and  $\epsilon_{\perp}$ ; splay  $K_{11}$  and bend  $K_{33}$  elastic constants; rotational viscosity  $\gamma_1$ ; and diffusion coefficients  $D_{\parallel}$  and  $D_{\perp}$  of a microsphere. Both  $\Delta n$  and  $\epsilon_{\parallel}$  decreases rapidly with increasing BC concentration, whereas  $\epsilon_{\perp}$  remains almost constant. At a shifted temperature (e.g.,  $T - T_{NI} = -10^{\circ}\text{C}$ ),  $K_{11}$  increases by  $\sim 50\%$  and  $K_{33}$  decreases by  $\sim 80\%$  compared to pure 5CB when the BC concentration is increased to  $\sim 43\%$  in the mixture. Viscosities parallel and perpendicular to the director,  $\eta_{\parallel}$ ,  $\eta_{\perp}$ , which are nearly equal to the Miesowicz viscosities  $\eta_2$  and  $\eta_3$ , respectively, were obtained by  $D_{\parallel}$  and  $D_{\perp}$  using the Stokes-Einstein relation. Both the viscosities at room temperature increase by 60 and 50 times, respectively, whereas  $\gamma_1$  increases by 180 times (at  $\sim 43\%$ ) compared to the corresponding values of pure 5CB. The stiffening of  $K_{11}$  and exorbitantly large enhancement in all the viscosities at a higher mol % of BC indicate that the viscoelastic properties are highly impacted by the presence of smectic clusters of BC molecules that results from the restricted free rotation of the molecules along the bow axis in the nematic phase. A possible attachment model of smectic type clusters of BC molecules surrounding the microparticle is presented.

DOI: [10.1103/PhysRevE.85.011702](https://doi.org/10.1103/PhysRevE.85.011702)

PACS number(s): 61.30.Eb, 61.30.Gd

**I. INTRODUCTION**

Low molecular weight liquid crystals made of rodlike molecules are commonly used for liquid crystal displays (LCDs). Usually multicomponent liquid crystal mixtures that exhibit a wide temperature range of the nematic phase are prepared to achieve optimum physical properties. Continuous effort over the decades to improve physical properties that enhances the display performance led to the discovery of many new liquid crystals with different molecular shapes and structures. In this context bent-core (BC) liquid crystals have created worldwide interests after the discovery of electro-optical switching in achiral BC compounds [1]. Many new phases of the so-called B phases and several new results based on the polarity and chirality are summarized in some excellent reviews [2–4]. To bring out just the effect of molecular shape on the physical properties, the BC nematic has been chosen for its simplicity, and consequently various new experimental results have been reported. For example, it is reported that BC nematic liquid crystals (NLCs) exhibit an opposite magnitude relation in splay-bend elastic constants [5,6], unusual electroconvection [7–9], giant flexoelectricity [10,11], large flow viscosity [12,13], the Kerr coefficient [14], and induced [15] and spontaneous biaxiality [16,17]. However, there are unresolved issues related to the alignment of the director in conventional liquid crystal cells [18] or phase biaxiality of pure BC NLCs [19]. Hence BC molecules have been added as dopants in some well characterized uniaxial rodlike compounds, and the effect of molecular shape on the physical properties of the mixtures is investigated. There are some interesting reports on the curvature elasticity of binary

mixtures of rodlike and BC molecules [20–26]. Dodge *et al.* showed that the addition of a small concentration of BC liquid crystals into a calamitic compound system reduces  $K_{33}$  by a factor of 2 or more [22,23], and they also developed a theoretical model. However theoretical predictions underestimated the experimental results. Kundu *et al.* reported anomalous trends in the temperature dependence of  $K_{11}$  and  $K_{33}$  in the nematic phase of mixtures of 4-n-octyloxy 4-cyanobiphenyl (8OCB) and a BC compound that does not exhibit nematic phase. The results were understood on the basis of their mutual orientations [20] in the presence of short-range smectic fluctuations. They also reported the evidence of polar clusters of BC molecules in the nematic phase of a binary mixture of rodlike and BC molecules [26]. Very recently we showed that  $K_{33}$  decreases significantly, whereas  $\Delta n$  and  $K_{11}$  remains invariant in binary mixtures due to the structural similarity of the rod molecule with one-half of the BC molecule [24].

All the experiments reported so far on BC nematic compounds exhibit the nematic phase much above the ambient temperature. Thus, studies on ambient-temperature BC NLCs or their mixtures with a calamitic compound could be rewarding from both the fundamental and application points of view. In this paper we report the measurement of birefringence  $\Delta n$ ; static dielectric constants  $\epsilon_{\parallel}$  and  $\epsilon_{\perp}$ ; splay  $K_{11}$  and bend  $K_{33}$  elastic constants; rotational viscosity  $\gamma_1$ ; diffusion coefficients  $D_{\parallel}$ ,  $D_{\perp}$  of a microsphere; and the corresponding viscosities  $\eta_{\parallel}$ ,  $\eta_{\perp}$  of ambient-temperature liquid crystal mixtures of BC and rodlike molecules. We show that the results are distinctly different than in previously studied mixtures. We find that the addition of BC to rodlike NLCs significantly increases the viscosities. High viscosities are disadvantageous and a matter of concern for room-temperature BC compounds to be useful for applications.

\*sdsp@uohyd.ernet.in

## II. EXPERIMENTAL

The experimental cells were made of two indium tin oxide (ITO) coated glass plates with circularly patterned electrodes. The plates were spin coated with polyimide (AL-1254), cured at 180 °C for 1 h, and rubbed antiparallely using a rubbing machine for planar or homogeneous alignment of the sample. In order to get homeotropic alignment, ITO plates were spin coated with polyimide (JALS-204) and cured at 200 °C. Glass-bead spacers with diameter  $\sim 5 \mu\text{m}$  were mixed with a UV curable adhesive. The cell thickness was measured by using a fibre optic spectrometer (Ocean Optics, HR-4000) with an accuracy of  $\pm 1\%$ . The empty cell was heated and filled with the sample in the isotropic phase. The textures were observed, and the phase transition temperatures of the mixtures were measured using a polarizing optical microscope (Nikon, LV100 POL) and a temperature controller (Instec, HCS 402). The perpendicular component of the static dielectric constant was measured in a planar cell using an impedance analyzer (Novocontrol, Alpha-A). In the case of a parallel component

of dielectric constant ( $\epsilon_{\parallel}$ ), the effective dielectric constant was measured from 0.01 to 20 V in steps of 0.02 V using an LCR meter (Agilent, 4980A). The experimental variation of a voltage dependent dielectric constant tends to saturate at high voltages. The linear part of the dielectric constant is plotted against  $1/V$  and extrapolated to  $1/V = 0$  to obtain  $\epsilon_{\parallel}$  at various temperatures. The measured values agree well with the measurements made in an independent cell. The voltage dependent optical retardation in the planar cell was measured simultaneously by a polarization modulation technique [27] using a photoelastic modulator (PEM-100, Hinds Instruments), a helium-neon laser (HT PS-Ec-1, Thor Labs), and a lock-in amplifier (Ametek, SR-7265). The modulation frequency was set to 50 kHz.  $K_{11}$  is obtained directly from the Fredericksz threshold voltage  $V_{th}$  and is given by  $K_{11} = \epsilon_o \Delta\epsilon (V_{th}/\pi)^2$ , where  $\Delta\epsilon = \epsilon_{\parallel} - \epsilon_{\perp}$  is the dielectric anisotropy. At strong surface anchoring condition, for voltages  $V$  above the threshold voltage  $V_{th}$ , the retardation  $\Delta\phi$  is given by the parametric equations [28]:

$$\frac{V}{V_{th}} = \frac{2}{\pi} \sqrt{1 + \gamma \sin^2(\phi_m)} \int_0^{\frac{\pi}{2}} \sqrt{\frac{1 + \kappa \sin^2(\phi_m) \sin^2(\psi)}{[1 + \gamma \sin^2(\phi_m) \sin^2(\psi)][1 - \sin^2(\phi_m) \sin^2(\psi)]}} d\psi, \quad (1)$$

$$\Delta\phi = 2\pi \frac{n_e d}{\lambda} \left( \frac{\int_0^{\frac{\pi}{2}} \sqrt{\frac{[1 + \gamma \sin^2(\phi_m) \sin^2(\psi)][1 + \kappa \sin^2(\phi_m) \sin^2(\psi)]}{[1 - \sin^2(\phi_m) \sin^2(\psi)][1 + \nu \sin^2(\phi_m) \sin^2(\psi)]}} d\psi}{\int_0^{\frac{\pi}{2}} \sqrt{\frac{[1 + \gamma \sin^2(\phi_m) \sin^2(\psi)][1 + \kappa \sin^2(\phi_m) \sin^2(\psi)]}{1 - \sin^2(\phi_m) \sin^2(\psi)}} d\psi} - \frac{n_o}{n_e} \right), \quad (2)$$

where  $d$  is the cell thickness, and the other terms of the reduced quantities are  $\gamma = (\epsilon_{\parallel}/\epsilon_{\perp}) - 1$ ,  $\kappa = (K_{33}/K_{11}) - 1$ , and  $\nu = (n_e^2/n_o^2) - 1$ .  $\phi$  is the  $z$ -dependent tilt angle, and  $\phi_m$  is the maximum tilt angle at the middle of the cell ( $z = d/2$ ) and is substituted with  $\sin(\phi) = \sin(\phi_m) \sin(\psi)$ . The sample retardation at higher voltage is fitted to the above equations by an iterative procedure to get the bend elastic constant  $K_{33}$  [20,29]. Experimentally measured  $K_{11}$  and  $K_{33}$  of pure 5CB agrees well with the previously reported values [30]. To verify the anchoring condition, we put the lower limit of the integration as a fit parameter  $\alpha$  in Eqs. (1) and (2) during fitting.  $\alpha$  was found to be less than  $1^\circ$  at all temperatures, implying the strong anchoring at the surfaces. Moreover we estimated the anchoring energy using the high electric field technique [31] in pure 5CB as well as in one mixture (20 mol %). The estimated anchoring energy is  $\sim 0.5 \times 10^{-4} \text{ J/m}^2$  in both the samples, suggesting the surface anchoring condition is sufficiently strong. It may be mentioned that the flexoelectric effect in unconventional liquid crystals could be significant and can influence  $K_{33}$  measurements. From voltage dependent dielectric measurements, it was shown by Brown *et al.* that it can slightly underestimate  $K_{33}$  when the flexoelectric effect is neglected [32]. Usually in voltage dependent dielectric measurement, the sample area is large ( $> 100 \times 10^{-6} \text{ m}^2$ ), the measured data is the average response over the whole sample area, and the accuracy in the measurement is somewhat less. In our electro-optic experiment we measured retardation over a small region ( $< 1 \times 10^{-6} \text{ m}^2$ ) using the photoelastic modulator and expected that such effect is minimal. Further

Kundu *et al.* [33] reported that the mixture of BC and rodlike compounds exhibit only homeotropic alignment because of a large positive self-energy due to a high flexoelectric coefficient at a higher concentration of BC molecules. In their study the individual compounds as well as the mixtures show smectic phases at lower temperature. In our samples no smectic phases are present, and we observe both homeotropic and planar alignment. Hence the flexoelectric contribution is expected to be negligibly small, and it can only affect the absolute accuracy in the measurements particularly at a very high concentration of BC molecules.

The rotational viscosity  $\gamma_1$  was measured in a planar cell by using a phase-decay-time measurement technique [34]. An arbitrary signal generator (Tektronix, AFG3102) was used to apply a sinusoidal voltage at a frequency of 4.111 kHz, and a photomultiplier tube (Hamamatsu, H6780-01) was used to measure the time dependent transmitted intensity. A small voltage  $V_b$  corresponding to the first maxima or minima was applied depending on transmission intensity such that the total phase retardation of the sample was  $n\pi$ , where  $n$  is an integer. At time  $t = 0$ , the bias voltage  $V_b$  was switched off and the relaxation transmission intensity change of the liquid crystal cell was measured with an oscilloscope (Tektronix, TDS 2012B). This procedure was repeated at various temperatures. The time dependent transmittance at a particular temperature in a planar cell is given by [34]

$$I(t) = I_o \sin^2\{[\Delta_{tot} - \delta(t)]/2\}, \quad (3)$$

where  $I_o$  is the maximum intensity change and  $\Delta_{\text{tot}}$  is the total phase difference. The optical phase difference  $\delta(t)$  for small director distortion can be approximated as  $\delta(t) = \delta_o \exp(-2t/\tau_o)$ , where  $\delta_o$  is total phase difference of a liquid crystal under bias voltage  $V_b$  that is not far from the Freedericksz threshold voltage  $V_{th}$ . In case  $\delta_o$  is close to  $n\pi$ ,  $\delta(t)$  becomes  $\delta(t) = \delta_o \exp(-4t/\tau_o)$ . The slope of the variation  $\ln[\delta_o/\delta(t)]$  with time  $t$  yields the relaxation time  $\tau_o$ . The rotational viscosity of liquid crystals is given by  $\gamma_1 = \tau_o K_{11} \pi^2 / d^2$ , where  $d$  is the thickness of liquid crystal sample.

To measure the diffusion coefficients  $D_{\parallel}$ ,  $D_{\perp}$ , we used a videomicroscopy technique where the Brownian motion of a tiny silica microsphere was tracked. The silica microspheres of diameter  $0.98 \mu\text{m}$  (Bangs Laboratories) were dispersed in a 0.5% water solution of octadecyldimethyl (3-trimethoxysilylpropyl) ammonium chloride (DMOAP) and mixed for several minutes. The microspheres were then rinsed with distilled water several times and dried for 30 min at  $120 \text{ }^\circ\text{C}$ . The dried microspheres were dispersed in the liquid crystal mixtures with an approximate concentration of 0.1%. Uniform colloidal dispersion was obtained by mechanical means like vortexing and sonication. The particles were observed under an inverted polarizing microscope (Nikon Eclipse, TE2000-U) with a water immersion microscope objective lens ( $100\times$ ). The Brownian motion of an isolated microsphere was video recorded for at least 300 s, and the position was determined with the help of an appropriate computer program with an accuracy of  $\pm 3 \text{ nm}$ . The histogram of the microparticle displacements is Gaussian, and the probability  $P$  that the particle would diffuse a certain distance  $s$  in the time interval  $\tau$  is given by

$$P = P_0 \exp\left(\frac{-s^2}{\Delta^2(\tau)}\right), \quad (4)$$

where  $\Delta(\tau)$  is the width of the Gaussian distribution and  $P_0$  is the normalization constant. The diffusion coefficients parallel and perpendicular to the director ( $D_{\parallel}$  and  $D_{\perp}$ ) of the thermal motion are obtained using the relation  $D_{\parallel,\perp} = \Delta_{\parallel,\perp} / 4\tau$ .

### III. RESULTS AND DISCUSSION

#### A. Samples and phase behavior

We studied various mixtures of the BC nematic compound 3-[4-(4-dodecyloxybenzylideneamino)benzoyloxy]-4-hexylphenyl 4-(4-dodecyloxybenzylideneamino)-benzoate and the calamitic nematic compound pentacyanobiphenyl (5CB). The chemical structures and the phase transition temperatures of the compounds are shown in Fig. 1(a). The synthesis and some preliminary characterization of the BC compound have already been reported [35]. Both the compounds exhibited the nematic phase at ambient temperature and antagonistically oriented resultant dipoles with respect to their long axes. The phase diagram of the binary mixtures is shown in Fig. 1(b). It is interesting to note that initially nematic-isotropic transition temperature  $T_{NI}$  is increasing with increasing mol % of the BC compound and reaches to a maximum at  $\sim 30 \text{ mol } \%$  of the BC compound before it decreases at a much higher mol %. Thus, the

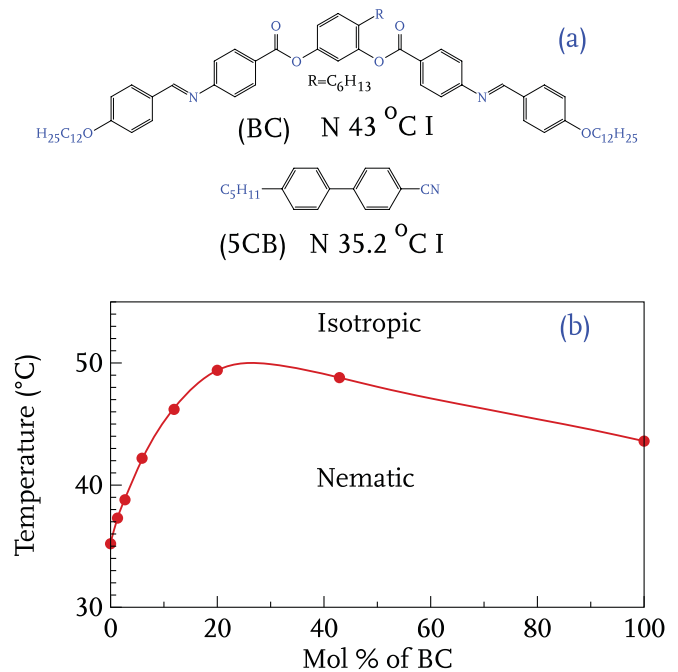


FIG. 1. (Color online) (a) Chemical structures of the compounds and the phase transition temperatures. (b) Phase diagram of the binary mixture.

nematic stability in the intermediate region of concentrations is enhanced in the mixture.

#### B. Optical and static dielectric constant measurements

In our physical measurements we restricted the mixing ratio of the BC up to  $\sim 43 \text{ mol } \%$  beyond which the dielectric anisotropy tends to change the sign and the viscosity is so high that the Brownian motion of the microparticle appears to be seized.

All the mixtures were studied carefully under the optical polarizing microscope, and it was found that all of them exhibit the uniaxial nematic phase. The temperature variation of  $\Delta n$  of the mixtures is shown in Fig. 2(a). In each mixture,  $\Delta n$  is increasing with decreasing temperature. At a fixed shifted temperature (i.e.,  $T - T_{NI}$ ),  $\Delta n$  is decreasing and tends to saturate at a much higher mol % of the BC compound. The temperature variation of  $\Delta n$  can be approximated by the Haller extrapolation formula [36],  $\Delta n = \Delta n_0 (1 - T/T^{**})^\beta$ , where  $\beta$ ,  $T^{**}$ , and the birefringence of the perfectly aligned sample,  $\Delta n_0$ , are the fit parameters. The fit parameters are listed in Table I.  $T^{**}$  is slightly higher than  $T_{NI}$ , and  $\beta$  is of the order of  $\sim 0.2$  instead of 0.5 as predicted by the mean field theory [37]. Similar values of  $\beta$  were also reported in many other calamitics [38] and in binary mixtures of calamitics and BC compounds [26]. The order parameter  $S$  of the long molecular axis was estimated using the relation  $S = \Delta n / \Delta n_0$ . The temperature variation of  $S$  of the mixtures are shown in Fig. 2(b).  $S$  increases in the nematic phase as the temperature is reduced.  $S$  decreases slightly from  $\sim 0.54$  to  $\sim 0.5$  when the mol % is increased to 5.9 and finally tends to saturate beyond it.

The variations of static dielectric constants as a function of shifted temperature are shown in Fig. 3. It is observed

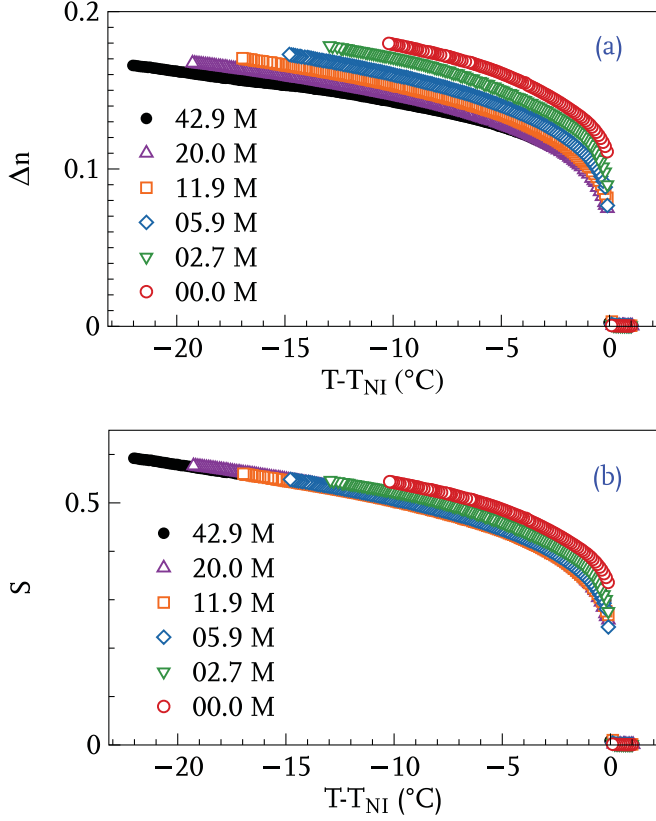


FIG. 2. (Color online) Temperature variation of (a) birefringence  $\Delta n$  and (b) estimated orientational order parameter  $S$  of the mixtures.

that the parallel component of dielectric constant  $\epsilon_{||}$  decreases rapidly with increasing mol % of the BC compound, whereas the perpendicular component  $\epsilon_{\perp}$  remains almost constant. The dielectric anisotropy is positive ( $\Delta\epsilon > 0$ ) and reduces significantly with increasing mol % of the BC compound. Since both the molecules have large dipole moments which are presumably oriented antagonistically in the nematic phase, i.e., in case of 5CB the dipole moment is parallel to the long axis, and in case of the BC molecule it is almost perpendicular to the bow axis. In the isotropic phases of the mixtures, it is fair to assume that the isotropic dielectric constant  $\epsilon_{iso} \propto \mu^2$ , where  $\mu$  is the mean-square effective molecular dipole moment [39]. The reduction in  $\epsilon_{iso}$  with increasing mol % of BC as observed indicates that the effective dipole moments in the isotropic phase is reduced. In the nematic phase the bow axis is assumed to be parallel to the director, and the molecules rotate freely

TABLE I. Fit parameters  $\Delta n_0$ ,  $T^{**}$ , and  $\beta$  obtained from Haller's extrapolation formula for the mixtures.

Mol %	$T_{NI}$ (K)	$T^{**}$ (K)	$\Delta n_0$	$\beta$
0	308.2	308.9	0.33	0.18
2.7	311.8	312.2	0.33	0.19
5.9	315.2	315.6	0.31	0.20
11.9	319.2	319.5	0.30	0.20
20	322.4	322.6	0.29	0.20
42.9	321.8	322.1	0.27	0.18

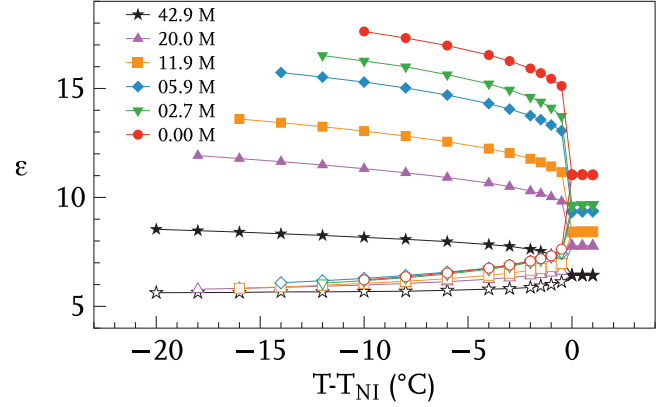


FIG. 3. (Color online) Temperature variations of dielectric constants  $\epsilon_{||}$  (closed symbols) and  $\epsilon_{\perp}$  (open symbols). Continuous lines are drawn as a guide to the eye.

about their long axes, so that the effect of transverse dipole moment is suppressed; as a result  $\epsilon_{\perp}$  remains constant. The longitudinal component of dipole moment of the BC molecule is much less than the 5CB molecule, and hence the longitudinal dipole moment per unit volume decreases with increasing mol % of BC molecules; as a result  $\epsilon_{||}$  can decrease.

### C. Splay and bend elastic constant measurements

The splay and bend elastic constants ( $K_{11}$ ,  $K_{33}$ ) were measured from the voltage dependent retardation in the planar cell as described earlier. Variations of the normalized retardation as a function of the applied voltage for a few mixtures are shown in Fig. 4. It is noticed that the Freedericksz threshold voltage increases with increasing mol % of the BC compound. The temperature variations of both  $K_{11}$  and  $K_{33}$  are shown in Fig. 5. In each mixture,  $K_{11}$  increases as the temperature is reduced [Fig. 5(a)], and at a shifted temperature,  $K_{11}$  increases with increasing mol % of the BC compound. In the case of  $K_{33}$  it is noticed that at a shifted temperature,  $K_{33}$  decreases rapidly [Fig. 5(b)] with increasing mol % of the BC compound. At 20 mol % of the BC compound,  $K_{33}$  is almost independent of temperature except very close to  $T_{NI}$ . Further, at  $\sim 43$  mol % of the BC compound,  $K_{33}$  increases initially and then decreases slightly as the temperature is reduced, showing a broad maximum

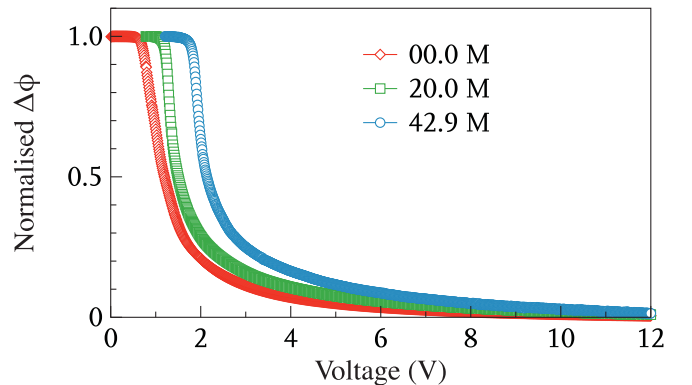


FIG. 4. (Color online) Voltage dependent normalized optical retardation  $\Delta\phi$  for the various mol % of the BC compound.

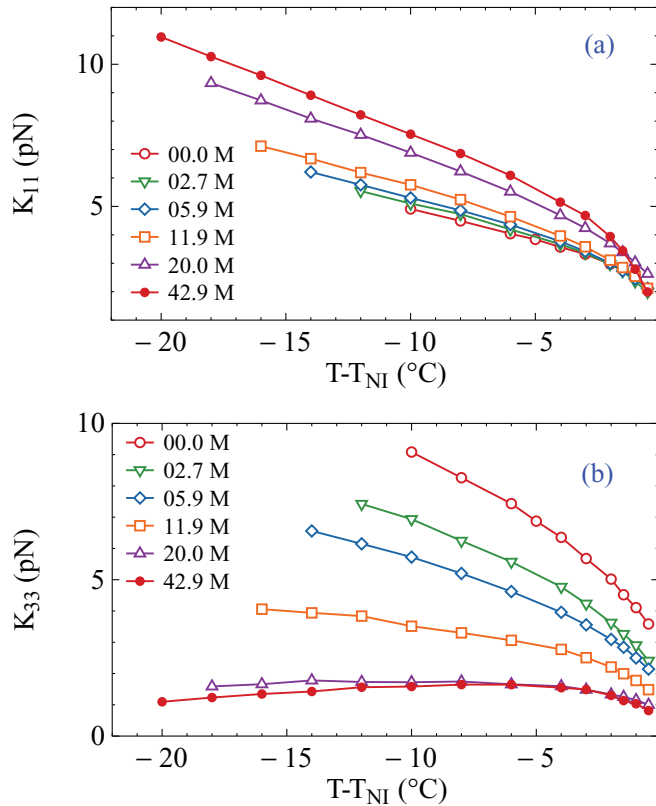


FIG. 5. (Color online) (a) Temperature variations of (a) splay  $K_{11}$  and (b) bend  $K_{33}$  elastic constants at the various mol % of the BC compound. Continuous lines are drawn as a guide to the eye.

approximately at  $T - T_{NI} \simeq -6^\circ\text{C}$ . In Fig. 6(a) variations of  $K_{11}$  and  $K_{33}$  at some shifted temperatures are presented with the mol % of the BC compound. It is observed that  $K_{11}$  increases by 50% with respect to pure 5CB at  $T - T_{NI} = -10^\circ\text{C}$ , whereas  $K_{33}$  decreases almost exponentially before it reaches to a minimum value when the mol % of the BC compound is increased to  $\sim 43\%$ . At a shifted temperature, e.g.,  $T - T_{NI} = -10^\circ\text{C}$ , the reduction is  $\sim 80\%$  compared to pure 5CB. The ratio of  $K_{33}/K_{11}$  as a function of the mol % at a few temperatures is shown in Fig. 6(b). The ratio reduces below 1 at  $\sim 5$  mol % of the BC compound and reaches to  $\sim 0.2$  at  $\sim 43$  mol %. Similar crossover was also reported in polymeric nematic liquid crystals, and it was shown that the ratio reduces to  $\simeq 0.83$  when the effective chain length to diameter ratio increases by a factor of 3 [40]. In the present binary system the ratio is significantly smaller ( $\sim 0.2$  at  $\sim 43$  mol %) and mainly due to the low  $K_{33}$  of the BC compound as seen in pure BC NLCs [5].

There have been a few reports on the measurements of  $K_{11}$  and  $K_{33}$  in binary mixtures of rodlike and BC molecules as mentioned earlier. In these studies it was found that both  $K_{11}$  and  $K_{33}$  decrease with increasing mol % of the BC compound, and the rate of decrement of  $K_{33}$  with the mol % of BC is several times faster than  $K_{11}$ . Very recently we found that  $K_{33}$  shows similar behavior, i.e., it decreases significantly, whereas  $K_{11}$  remains almost constant in the binary mixtures due to the structural similarity of the rod molecule with one-half of the BC molecule [24]. The increase of  $K_{11}$  with increasing mol %

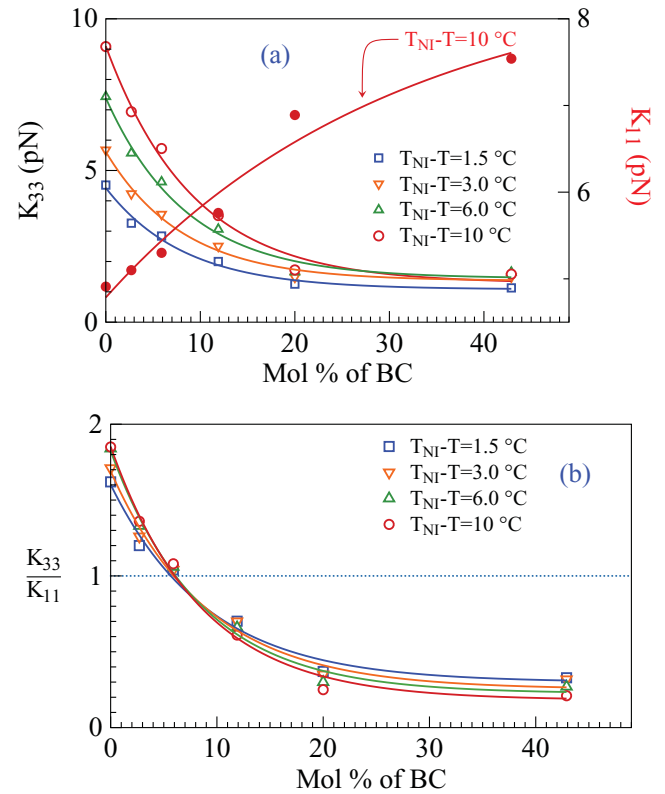


FIG. 6. (Color online) (a) Variation of  $K_{11}$  (closed circles) and  $K_{33}$  (open symbols) with the mol % of the BC compound at various shifted temperatures and (b) variation of  $K_{33}/K_{11}$  with the mol % of the BC compound.

of BC was reported recently [41], as observed in the present study. The reduction in  $K_{33}$  is explained due to the coupling of the bent shape of the molecules with the bend distortion which results in reduction of bend stress. The anomalous temperature dependence of  $K_{33}$  at  $\sim 43$  mol % (i.e., it decreases with decreasing temperature) is due to the enhanced orientational order  $S$  of the BC molecules. A similar observation at a higher mol % of BC was also reported by Kundu *et al.* [20]. It suggests that the coupling of the *bent shape* of the molecule with the bend distortion is stronger at higher  $S$ . To gain more insight on the relationship between the order parameter and elastic constants, we plotted the variations of  $K_{11}$  and  $K_{33}$  as a function of  $\Delta n$  in Fig. 7. The experimental data are fitted with  $K_{ii} \propto \Delta n^x$ , where  $x$  is a fit parameter. The fit parameters are listed in Table II. It is observed that the exponent  $x$  for  $K_{11}$  is 2 up to 11.9 mol % and is consistent with the prediction of mean field theory ( $K_{11} \propto S^2$ ). It increases to 2.8 at  $\sim 43$  mol %. A similar value of  $x$  ( $\simeq 2.9$ ) was reported in the case of pure BC NLC [5]. On the other hand the exponent  $x$  for  $K_{33}$  is  $\sim 2$  up to 5.9 mol % and starts decreasing beyond this concentration (Table II). It clearly indicates that the coupling of bent shape with the bend distortion is significant beyond 5.9 mol % of the BC compound. At a higher concentration (particularly at 20 and  $\sim 43$  mol %),  $K_{33}$  initially increases and finally decreases with increasing  $\Delta n$  showing a maxima at  $\Delta n \sim 0.14$ . The initial increase is due to the increasing orientational order  $S$  as expected. However with increasing  $S$  the coupling with bend distortion also gets stronger; as a result  $K_{33}$  starts to decrease.

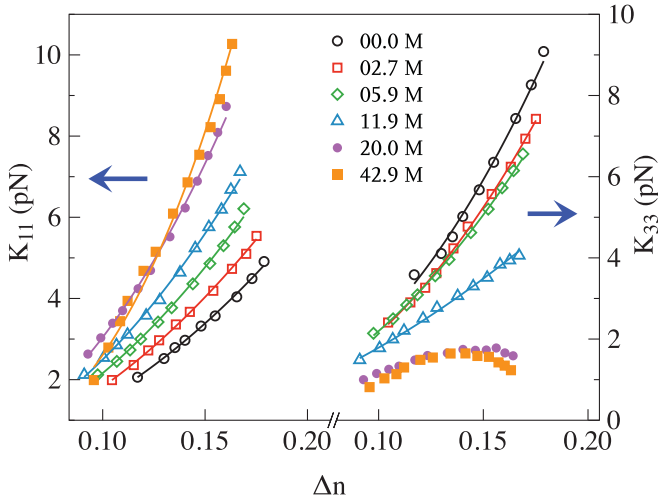


FIG. 7. (Color online) (a) Variations of  $K_{11}$  and  $K_{33}$  with  $\Delta n$  at the various mol % of the BC compound. Continuous lines are fit to the equation  $K_{ii} \propto \Delta n^x$ .

For the enhancement of  $K_{11}$ , at least two considerations can be made.  $K_{11}$  can increase in the mixture due to an increase in  $S$  as predicted in the mean field theory ( $K_{11} \propto S^2$ ). On the contrary, we observe [Fig. 2(b)] that  $S$  decreases slightly with increasing mol % of the BC compound. Thus the stiffening of  $K_{11}$  can not be attributed to the enhancement of  $S$ . Another possible explanation is based on the evolution of the transverse correlation (i.e., along the short axis) of two or more BC molecules that is developed due to the restricted free rotation along the long axis. This can lead to the formation of smectic cybotactic clusters of a few BC molecules. The larger exponent (i.e.,  $x > 2$ ) for  $K_{11}$  at a higher mol % of BC may be a pointer to the existence of a short axis correlation. There are several reports suggesting the formation of smectic clusters in BC NLCs or in binary mixtures of rod and BC molecules [26,42,43]. It is possible that the enhancement of  $K_{11}$  is due to the presence of such clusters whose corresponding elastic constants are expected to be larger. The number density and size of these clusters can increase with an increasing concentration of BC molecules.

**D. Viscosity measurements**

Finally we discuss the measurements of diffusion coefficients  $D_{||}$  and  $D_{\perp}$  of the microsphere, where the subscripts refer to the direction in relation to the director and rotational viscosity  $\gamma_1$  of the mixtures. The microparticle undergoes

TABLE II. Fit parameters obtained from  $K_{ii} \propto \Delta n^x$  for the mixtures.

Mol %	$\simeq x$ for $K_{11}$	$\simeq x$ for $K_{33}$
0	2.0	2.2
2.7	2.0	2.2
5.9	2.0	2.1
11.9	2.0	1.7
20	2.2	
42.9	2.8	

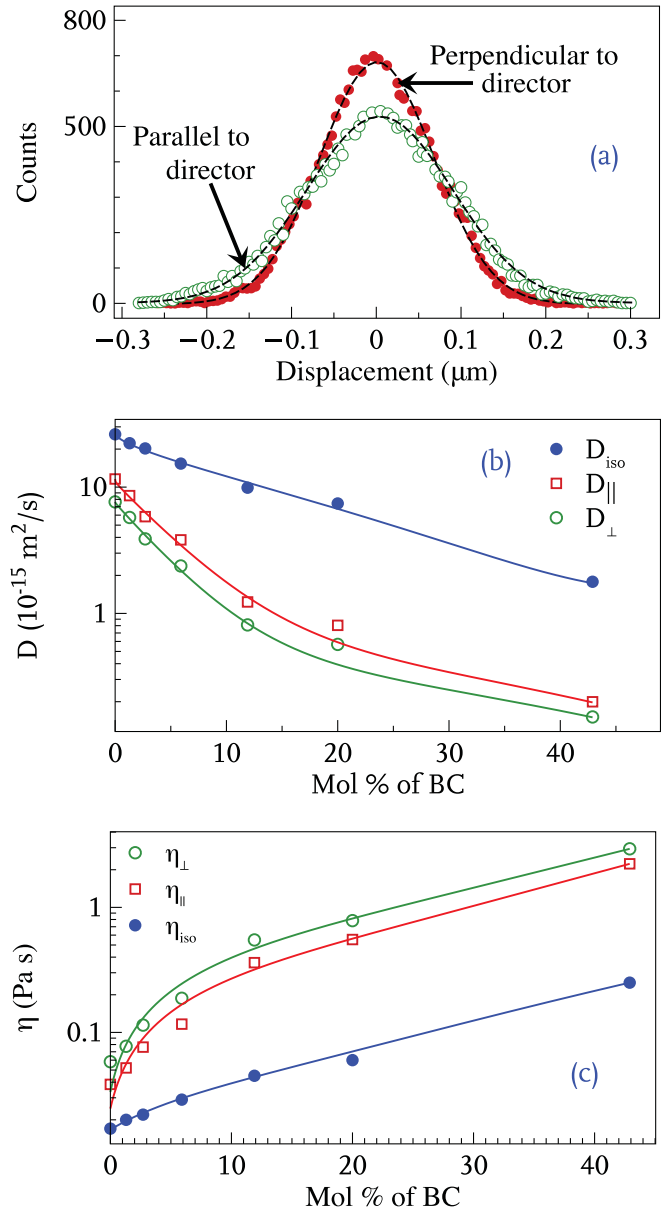


FIG. 8. (Color online) (a) Typical histograms of the displacements of a microsphere of diameter  $0.98 \mu\text{m}$  in direction parallel and perpendicular to the nematic director at room temperature for the mixture with 10 mol % of the BC compound. Dotted lines are fit Eq. (4) to the corresponding data. (b) Variations of diffusion coefficients parallel  $D_{||}$  and perpendicular  $D_{\perp}$  to the director with the mol % of the BC compound at  $25 \text{ }^\circ\text{C}$  (open symbols) and  $T_{NI} + 5 \text{ }^\circ\text{C}$  (closed symbol). (c) Estimated viscosities using the Stokes-Einstein relation. Continuous lines are drawn as a guide to the eye.

Brownian motion and the histogram of the displacement has a Gaussian shape. Typical histograms, i.e., the variation of the displacement of a colloid in a particular interval over a specified time (counts) along and perpendicular to the director in a planar aligned cell, are shown in Fig. 8(a). The variations of diffusion coefficients  $D_{||}$  and  $D_{\perp}$  with the mol % of the BC compound are shown in Fig. 8(b). The isotropic diffusion coefficient  $D_{\text{iso}}$  is significantly higher than  $D_{||}$  and  $D_{\perp}$  of the nematic phase, and all of them decrease as the mol % of the BC compound is increased. The corresponding

viscosities can be obtained from the Stokes-Einstein equation  $\eta_{||,\perp} = k_B T / (6\pi r D_{||,\perp})$ , where  $r$  is the radius of the microparticle. From the experimental arrangement we can expect the relationship  $\eta_{||} \simeq \eta_2$  and  $\eta_{\perp} \simeq \eta_3$ , where  $\eta_2, \eta_3$  are the Miesowicz viscosities with flow direction parallel and perpendicular to the director, respectively.

It may be pointed out that a dipole defect is associated with each microparticle. Hence the effective hydrodynamic radius of the microparticle could be slightly larger than the actual size. However, it appears not to affect the measurements, since the estimated values of  $\eta_{||}$  and  $\eta_{\perp}$  for pure 5CB at room temperature in a planar cell agree well with Miesowicz viscosities  $\eta_2$  and  $\eta_3$ , respectively. The estimated viscosities against the mol % of BC are shown in Fig. 8(c). It is noticed that the isotropic viscosity  $\eta_{iso}$  increases only slightly with the mol % of the BC compound. This is perhaps due to the molecular size effect of BC molecules in the mixtures. In all the mixtures  $\eta_{||} < \eta_{\perp}$  as expected, and both of them increase relatively more rapidly than  $\eta_{iso}$  with the mol % of the BC compound [Fig. 8(c)]. For example,  $\eta_{||}/\eta_{iso} \simeq 12$  and  $\eta_{\perp}/\eta_{iso} \simeq 9$  at  $\sim 43$  mol % of the BC compound at ambient temperature. Such a large enhancement in Miesowicz viscosities with increasing mol % of the BC compound indicates the existence of clusters as mentioned earlier. Experimental evidence on the existence of such clusters has been revealed in various other experiments [26,42–47].

We measured the rotational viscosity  $\gamma_1$  of the mixtures at various temperatures which is also expected to be influenced by the presence of cybotactic clusters. The variation of  $\gamma_1$  for the mixtures are shown in Fig. 9; Fig. 9(a) shows the shifted-temperature dependence of  $\gamma_1$  for a few mixtures of the different mol % of the BC compound, and Fig. 9(b) shows the BC concentration dependence at a few shifted temperatures. It is found that  $\gamma_1$  increases rapidly with the mol % of the BC compound. For example, at  $T - T_{NI} = -10^\circ\text{C}$ , it increases almost by a factor of 180 when the mol % of the BC compound is increased to  $\sim 43$  in the mixtures. Measurement of  $\gamma_1$  with the phase-decay technique and flow viscosities using a pulsed magnetic field of a few pure BC NLCs have been reported recently [13,48,49]. It was reported that the ratio  $\Gamma = \gamma_1/\eta$  is significantly less for the BC compound ( $\Gamma \sim 0.02$ ) than the calamitic liquid crystals mainly due to the large value of flow viscosity [48]. On the contrary, in the present study we observe that  $\Gamma$  increases remarkably with the mol % of the BC compound compared to pure 5CB. For example, in pure 5CB,  $\Gamma_{\perp} = \gamma_1/\eta_{\perp} \sim 1$  and  $\Gamma_{||} = \gamma_1/\eta_{||} \sim 1.5$  and increase to 12 and 16, respectively [Fig. 9(b), inset] when the mol % of the BC compound is increased to  $\sim 43$  in the mixture. It may be noted that all viscosities  $\gamma_1, \eta_2,$  and  $\eta_3$  increase with the mol % of the BC compound, but the rate of increment of  $\gamma_1$  is much faster than the other two.

Such exorbitantly large increase in  $\gamma_1$  can not be accounted for by the increase of the mol % of BC molecules with large molecular weight alone in the mixtures. The relatively faster enhancement of  $\gamma_1$  with respect to the Miesowicz viscosities can be attributed to the presence of smectic clusters of BC molecules. In the present mixtures both the compounds do not have any smectic phases. Nevertheless the smectic clusters are formed inherently due to the highly restricted free rotation of the BC molecules along the bow axis. Further, the BC molecules presumably align perpendicularly on the surface of the microparticle due to the DMOAP coating. In that case the steric barrier and partial pinning of the molecules on the microsphere's surface prevent free rotation of the BC molecules along the bow axes, and a few BC molecules

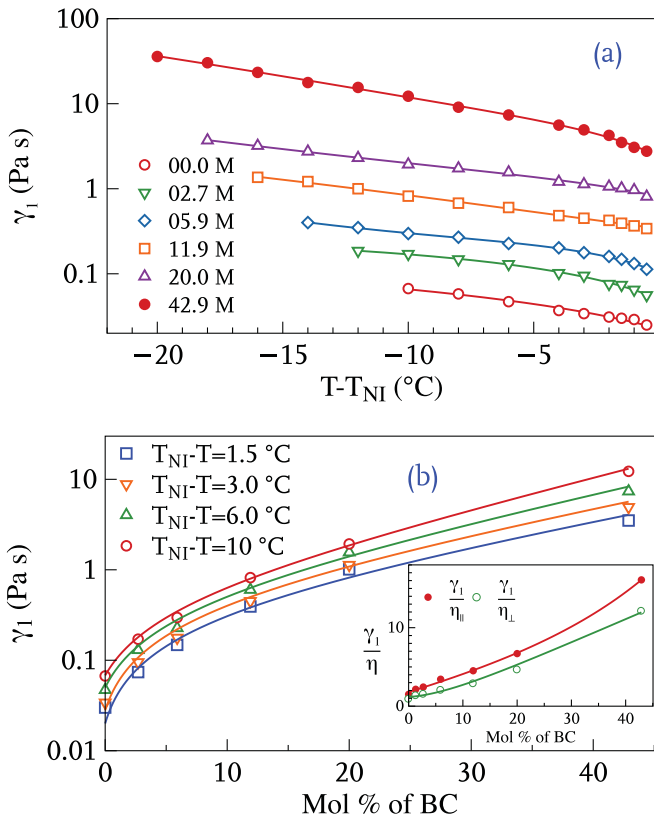


FIG. 9. (Color online) (a) Variation of the rotational viscosity  $\gamma_1$  of various mixtures as a function of the shifted temperature. (b) Variation of the  $\gamma_1$  with the mol % of the BC compound at a few shifted temperatures. Ratio of  $\gamma_1/\eta_{||,\perp}$  with the mol % of the BC compound is also shown in the inset. Continuous lines are drawn as a guide to the eye.

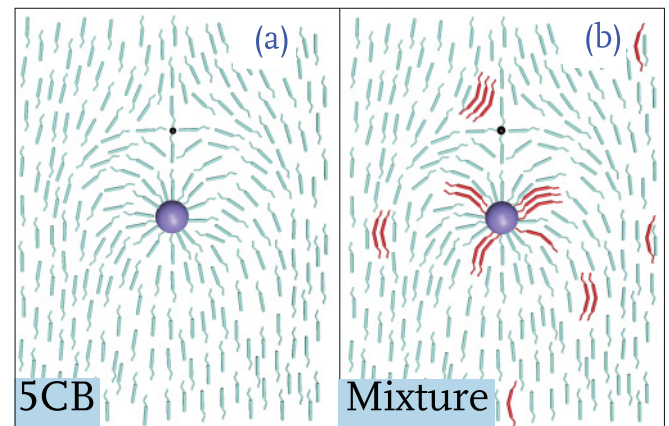


FIG. 10. (Color online) Schematic representations of the director orientation around a microparticle with a dipole defect (a) in rodlike molecules and (b) in the mixture. The small dot above the microparticle is the center of the dipole defect. Note the attachment of a few clusters of BC molecules surrounding the microparticle.

can form smectic clusters or permanent layers at the surface which in principal can reduce the Brownian motion of the microparticle and can increase the Miesowicz viscosities. Schematic representations of such clusters surrounding the microparticle with dipole defects are shown in Fig. 10. It may be mentioned that no Brownian motion was observed in the pure BC compound at room temperature. This is perhaps due to the very large viscosities and presence of a few smectic layers surrounding the microparticle.

#### IV. CONCLUSIONS

In conclusion, measurements of optical, dielectric, and viscoelastic properties of room temperature nematic liquid crystals with rodlike and BC molecules have shown the following interesting results: (1) a mutual alignment of the bow axis in 5CB is such that the effective dipole moment in the isotropic and in the nematic phases parallel to the director is reduced; (2) a significant stiffening of splay and large softening of bend elastic constants; (3) a large reduction in both the diffusion coefficients in the nematic phase compared to the isotropic phase and hence an unprecedented increase in

the Miesowicz viscosities; and (4) a two order of magnitude enhancement in the rotational viscosity with increasing mol % of the BC compound. The stiffening of  $K_{11}$  and extraordinarily large viscosities are attributed to the presence of smectic clusters of BC molecules in the mixtures. Present studies suggest that an ambient-temperature BC nematic could be advantageous as a dopant for optimizing the birefringence, dielectric constants, and elastic properties of low molecular weight liquid crystals, but the enhanced viscosities in the mixtures are highly disadvantageous as well as a matter of concern and have to be reduced for practical application.

#### ACKNOWLEDGMENTS

S.D. gratefully acknowledges the support from UGC-CAS School of Physics and DST, Government of India, Project No. SR/NM/NS-134/2010 for financial support. P.S. acknowledges support through a CSIR-UGC fellowship. V.S.R.J acknowledges (EC)7OP Marie Curie ITN Project HIERARCHY Grant No. PITN-GA-2008-215851 and the Slovenian Research Agency (ARRS) Contract No. P1-0099. We thank Professor J. Mieczkowski for the BC compound.

- 
- [1] T. Niori, T. Sekine, J. Watanabe, T. Furukawa, and H. Takezoe, *J. Mater. Chem.* **6**, 1231 (1996).
- [2] H. Takezoe and Y. Takanishi, *Jpn. J. Appl. Phys.* **45**, 597 (2006).
- [3] J. Etxebarria and M. B. Ros, *J. Mater. Chem.* **18**, 2919 (2008).
- [4] R. A. Reddy and C. Tschierske, *J. Mater. Chem.* **16**, 907 (2006).
- [5] P. Sathyanarayana, M. Mathews, Q. Li, V. S. S. Sastry, B. Kundu, K. V. Le, H. Takezoe, and S. Dhara, *Phys. Rev. E* **81**, 010702(R) (2010).
- [6] M. Majumdar, P. Salamon, A. Jakli, J. T. Gleeson, and S. Sprunt, *Phys. Rev. E* **83**, 031701 (2011).
- [7] D. Wiant, J. T. Gleeson, N. Eber, K. Fodor-Csorba, A. Jakli, and T. Toth-Katona, *Phys. Rev. E* **72**, 041712 (2005).
- [8] S. Tanaka, S. Dhara, B. K. Sadashiva, Y. Shimbo, Y. Takanishi, F. Araoka, K. Ishikawa, and H. Takezoe, *Phys. Rev. E* **77**, 041708 (2008).
- [9] S. Tanaka, H. Takezoe, N. Eber, K. Fodor-Csorba, A. Vajda, and A. Buka, *Phys. Rev. E* **80**, 021702 (2009).
- [10] J. Harden, B. Mbanga, N. Eber, K. Fodor-Csorba, S. Sprunt, J. T. Gleeson, and A. Jakli, *Phys. Rev. Lett.* **97**, 157802 (2006).
- [11] K. V. Le, F. Araoka, K. F. Csorba, K. Ishikawa, and H. Takezoe, *Liq. Cryst.* **36**, 1119 (2009).
- [12] E. Dorjgotov, K. Fodor-Csorba, J. T. Gleeson, S. Sprunt, and A. Jakli, *Liq. Cryst.* **35**, 149 (2008).
- [13] P. Sathyanarayana, T. Arun Kumar, V. S. S. Sastry, M. Mathews, Q. Li, H. Takezoe, and S. Dhara, *Appl. Phys. Express.* **3**, 091702 (2010).
- [14] S. Dhara, F. Araoka, M. Lee, K. V. Le, L. Guo, B. K. Sadashiva, K. Song, K. Ishikawa, and H. Takezoe, *Phys. Rev. E* **78**, 050701(R) (2008).
- [15] J. A. Olivares, S. Stojadinovic, T. Dingemans, S. Sprunt, and A. Jakli, *Phys. Rev. E* **68**, 041704 (2003).
- [16] B. R. Acharya, A. Primak, and S. Kumar, *Phys. Rev. Lett.* **92**, 145506 (2004).
- [17] L. A. Madsen, T. J. Dingemans, M. Nakata, and E. T. Samulski, *Phys. Rev. Lett.* **92**, 145505 (2004).
- [18] A. Kumar, K. V. Le, J. K. Kim, H. Takezoe, and S. Dhara, *Liq. Cryst.* **38**, 917 (2011).
- [19] B. Senyuk, H. Wonderly, M. Mathews, Q. Li, S. V. Shiyankovskii, and O. D. Lavrentovich, *Phys. Rev. E* **82**, 041711 (2010).
- [20] B. Kundu, R. Pratibha, and N. V. Madhusudana, *Phys. Rev. Lett.* **99**, 247802 (2007).
- [21] R. Pratibha, N. V. Madhusudana, and B. K. Sadashiva, *Science* **288**, 2184 (2000).
- [22] M. R. Dodge, C. Rosenblatt, R. G. Petschek, M. E. Neubert, and M. E. Walsh, *Phys. Rev. E* **62**, 5056 (2000).
- [23] M. R. Dodge, R. G. Petschek, C. Rosenblatt, M. E. Neubert, and M. E. Walsh, *Phys. Rev. E* **68**, 031703 (2003).
- [24] P. Sathyanarayana, B. K. Sadashiva, and S. Dhara, *Soft Matter* **7**, 8556 (2011).
- [25] P. Salamon, N. Eber, A. Buka, J. T. Gleeson, S. Sprunt, and A. Jakli, *Phys. Rev. E* **81**, 031711 (2010).
- [26] B. Kundu, R. Pratibha, and N. V. Madhusudana, *Eur. Phys. J. E* **31**, 145 (2010).
- [27] T. C. Oakberg, *SPIE Proceedings* **3121**, 19 (1997).
- [28] G. Barbero and L. R. Evangelista, *An Elementary Course on the Continuum Theory for Nematic Liquid Crystals* (World Scientific, Singapore, 2000).
- [29] S. W. Morris, P. Palffy, and D. A. Balzarini, *Mol. Cryst. Liq. Cryst.* **139**, 263 (1986).
- [30] A. Bogi and S. Faetti, *Liq. Cryst.* **28**, 729 (2001).
- [31] H. Yokoyama and H. A. Sprang, *J. Appl. Phys.* **57**, 4520 (1985).
- [32] C. V. Brown and N. J. Mottram, *Phys. Rev. E* **68**, 031702 (2003).
- [33] B. Kundu, A. Roy, R. Pratibha, and N. V. Madhusudana, *Appl. Phys. Lett.* **95**, 081902 (2009).
- [34] S. T. Wu and C. S. Wu, *Phys. Rev. A* **42**, 2219 (1990).

- [35] J. Matraszek, J. Mieczkowski, J. Szydowska, and E. Gorecka, *Liq. Cryst.* **27**, 429 (2000).
- [36] I. Hallar, *Prog. Solid-State Chem.* **10**, 103 (1975).
- [37] P. G. de Gennes and J. Prost, *The Physics of Liquid Crystals*, 2nd ed. (Clarendon Press, Oxford, 1993).
- [38] S. Dhara and N. V. Madhusudana, *Eur. Phys. J. E* **13**, 401 (2004).
- [39] H. Froehlich, *Theory of Dielectrics*, 2nd ed. (Clarendon Press, Oxford, 1968).
- [40] S. D. Lee and R. B. Meyer, *Phys. Rev. Lett.* **61**, 2217 (1988).
- [41] S. T. Hur, M. J. Gim, H. J. Yoo, S. W. Choi, and H. Takezoe, *Soft Matter* **7**, 8800 (2011).
- [42] C. Baily, K. Fodor-Csorba, J. T. Gleeson, S. N. Sprunt, and A. Jakli, *Soft Matter* **5**, 3618 (2009).
- [43] S. Stojadinovic, A. Adorjan, S. Sprunt, H. Sawade, and A. Jakli, *Phys. Rev. E* **66**, 060701(R) (2002).
- [44] O. Francescangeli and E. T. Samulski, *Soft Matter* **6**, 2413 (2010).
- [45] S. H. Hong, R. Verduzco, J. C. Williams, R. J. Twieg, E. DiMasi, R. Pindak, A. Jakli, J. T. Gleeson, and S. Sprunt, *Soft Matter* **6**, 4819 (2010).
- [46] O. Francescangeli, F. Vita, C. Ferrero, T. Dingemans, and E. T. Samulski, *Soft Matter* **7**, 895 (2011).
- [47] M. Cifelli and V. Domenici, *Phys. Chem. Chem. Phys.* **9**, 1202 (2007).
- [48] E. Dorjgotov, K. Fodor-Csorba, J. T. Gleeson, S. Sprunt, and A. Jakli, *Liq. Cryst.* **35**, 149 (2008).
- [49] P. Tadapatri, U. S. Hiremath, C. V. Yelamaggad, and K. S. Krishnamurthy, *J. Phys. Chem. B* **114**, 1745 (2010).